Human mesenchymal stem cells response to multi-doped silicon-strontium calcium phosphate coatings

Cosme Rodríguez-Valencia, Iago Pereiro, Rogelio P Pirraco, Miriam López-Álvarez, Julia Serra, Pío González, Alexandra P Marques and Rui L Reis

J Biomater Appl published online 25 October 2013
DOI: 10.1177/0885328213510056

Original Article

JOURNAL OF
biomaterials
applications

Journal of Biomaterials Applications
0(0) 1–11

DOI: 10.1177/0885328213510056
jba.sagepub.com
SAGE

Human mesenchymal stem cells response to multi-doped silicon-strontium calcium phosphate coatings

Cosme Rodríguez-Valencia[1], Iago Pereiro[1], Rogelio P Pirraco[2,3], Miriam López-Álvarez[1], Julia Serra[1], Pío González[1], Alexandra P Marques[2,3] and Rui L Reis[2,3]

Abstract

The search for apatitic calcium phosphate coatings to improve implants osteointegration is, nowadays, preferentially focused in the obtaining of compositions closer to that of the inorganic phase of bone. Silicon and strontium are both present in trace concentrations in natural bone and have been demonstrated, by separate, to significantly improve osteoblastic response on calcium phosphate bioceramics. This work aims the controlled and simultaneous multi-doping of carbonated calcium phosphate coatings with both elements, Si and Sr, by pulsed laser deposition technique and the biological response of human mesenchymal stem cells to them. A complete physicochemical characterization has been also performed to analyze the coatings and significant positive effect was obtained at the osteogenic differentiation of cells, confirming the enormous potential of this multi-doping coating approach.

Keywords

Multi-doped coatings, pulsed laser deposition, calcium phosphate, strontium, silicon, human bone marrow-derived mesenchymal stem cells differentiation

Introduction

In the last decades, different biomaterials have been designed, produced and evaluated with the aim of improving human health and the quality of life. Within these materials, titanium alloys are mostly used in orthopaedic prosthesis and dental implants mainly due to their excellent mechanical properties. However, when implanted in vivo, these metal alloys show a very poor capability of promoting the bonding between the implant surface and the surrounding bone, which results in a destabilization of the prosthesis at the medium-long term.[1] Related with this interface interaction, it has been proven that the long-term performance of the prosthesis depends directly on their surface properties.[2,3]

The coating of metallic prosthesis with calcium phosphates (CaP) is considered one of the approaches to avoid that destabilization[4] and to enhance the implant durability, as concluded Voigt and Mosier[5] in a meta-analysis of total knee arthroplasties coated with hydroxyapatite against un-coated. Although nowadays there is no consensus regarding whether there is a clear clinical benefit on the application of this CaP coatings on titanium implant devices, it has been accepted that their application is at least advantageous to enhance bone formation around the implants, to contribute to cementless fixation and thus to improve clinical success at an early stage after implantation.[6] The evaluation of

[1]New Materials Group, Applied Physics Dpt., Institute of Biomedical Research of Vigo (IBIV), University of Vigo, Spain
[2]3B's Research Group – Biomaterials, Biodegradables and Biomimetics, University of Minho, Headquarters of the European Institute of Excellence on Tissue Engineering and Regenerative Medicine, Guimarães, Portugal
[3]ICVS/3B's Laboratório Associado, PT Government Associated Laboratory, Braga, Portugal

Corresponding author:
Miriam López Álvarez, New Materials Group, Applied Physics Dpt., School of Industrial Engineering, Campus Lagoas-Marcosende, University of Vigo, 36310 Vigo, Spain.
Email: miriammsd@uvigo.es

CaP coatings is still of great interest given the proven results at osteogenesis promotion as, for instance, in the work published by Ripamonti et al.[7] presenting osteoinductive hydroxyapatite-coated titanium implants where concavities of 1600 μm were performed on the substrate to propose an in vivo bioreactor-like process, where the hydroxyapatite dissolution process were involved.

Plasma spraying is at present the most commonly used technique to coat metallic implants. Nevertheless, this technique presents difficulties in the control of the final coating composition and requires a considerable thickness in the coatings.[8–10] The pulsed laser deposition (PLD) technique has been proposed as an alternative to plasma spray, given that this method allows the formation of films with controlled thickness, morphology and composition.[10–13] This technique can produce CaP coatings with diverse compositions and crystallinities and thin coatings, which are advantageous for high fatigue resistance.[6] García-Sanz et al.[8] found that the bonding strength between CaP coating (by PLD) and the substrates was 58 MPa, which was higher than the value obtained in plasma-sprayed coatings. Thus, PLD technique allows the formation of films with controlled thickness, morphology and composition.[10–13] Moreover CaP coatings produced by PLD have been proven to enhance the cell proliferation rate and the level of differentiation both in vitro[14] and in vivo.[15]

To improve the bioactive properties of metallic implants coated with CaP, and thus reduce the post-operatory recovery of the patient, the surface composition should be as similar as possible to the surrounding bone tissue. Thus, in this study, two elements, Si and Sr, were chosen as the main doping of the CaP coatings.

Silicon (Si) is known to play an important role in the development of the connective tissue, especially in the early stages of bone formation, as demonstrated by Carlisle in 1980.[16] Its deficiency is correlated with a deficient production of collagen which leads to a reduction in bone proliferation and the occurrence of deformations and injuries.[16] Si has also been shown to play an important role in the union of different polysaccharides[17] and the induction of osteoblastic genes that control cell proliferation and adhesion.[18] Furthermore, treatments with Si have been successful in augmenting the bone density of osteoporotic patients.[19]

Strontium (Sr) is another element found in trace concentrations in the skeleton, found to be in the range of 0.01–0.02 wt% in human bones,[20,21] only 0.035 of their Ca content,[22] and this content is higher in the regions of high metabolic turnover. Recently, there has been an increasing awareness of the biological role of this element. In vitro studies have shown that the presence of Sr increases the number of osteoblasts and reduces the number and activity of osteoclasts. On the other hand, in vivo studies have shown an increase in bone mass and strength and a reduction of the natural bone resorption,[23–25] leading to its approval in many countries as a treatment for osteoporotic patients in the form of strontium ranelate.

One of the advantages of the PLD technique is that it allows the incorporation of different elements into the CaP coatings, either as a lattice substitution or as an interstitial doping, and this in a relatively simple way. In particular, following the procedure of mixture, compaction and subsequent ablation of powders, Si has been shown to be incorporated into CaP by PLD from a variety of sources,[26] and of particular interest is its possibility of incorporation from diatomaceous earth, a naturally occurring siliceous sedimentary rock that contains silica in a 92 at.% but also small percentages of Fe, K, Mg, Na and P among other elements. On the other hand, Sr has recently been shown to be incorporated into the CaP coatings with same technique with the use of strontium carbonate ($SrCO_3$) powders as a precursor,[27] being this a chemically stable source of both Sr and carbonate groups. It is, however, the hypothetical combination of these different experiences that would open the possibility for obtaining the desired multi-doped CaP coatings.

While, as seen, some studies have proven the possibility of obtaining doped CaP coatings by laser ablation, the literature on multi-doped CaP films remain scarce. The objective of this study has hence been to obtain multi-doped CaP coatings on metallic substrates containing both Si and Sr, being diatomaceous earth and strontium carbonate, the sources that have already been proven in the production of doped CaP coatings with the PLD technique.[26,27] Once physicochemical characterization studies were performed for coatings fabricated with a range of Si and Sr concentrations, we have selected a concentration for evaluation of cell attachment, proliferation and differentiation of human bone marrow-derived mesenchymal stem cells (hBMSCs).

Materials and methods

Synthesis of CaP and Si-Sr-CaP coatings

The PLD target disks, with a mass of 2 g and a diameter of 20 mm, were fabricated with the homogeneous mixture of commercial carbonated HA (Plasma Biotal Captal-1R), diatomaceous earth (provided by CIIMAR, Interdisciplinary Centre of Marine and Environmental Research, University of Porto, Portugal) and $SrCO_3$ (Sigma 204455) powders and the subsequent application of pressure (30 MPa).

Table 1. Designation of the coatings with the atomic percentage of Si and Sr in the target material.

at.% Si	at.% Sr	Coating
0	0	Si0Sr0
2.5	0	Si2.5Sr0
2.5	2.5	Si2.5Sr1.75
2.5	5.0	Si2.5Sr2.5
2.5	7.5	Si2.5Sr5.0
2.5	10.0	Si2.5Sr7.5

Six targets with different concentrations were fabricated: a reference target of pure carbonated HA and five targets containing a constant 2.5 at.% Si (considering a 92.3 at.% of SiO_2 in the diatomaceous earth) and an at.% Sr of 0, 1.75, 2.5, 7.5 and 10.0. Targets were labeled as Si0Sr0, Si2.5Sr0, Si2.5Sr1.75, Si2.5Sr2.5, Si2.5Sr5.0 and Si2.5Sr7.5 (Table 1). Titanium grade 5 discs (SMP, Barcelona, Spain) with dimensions of 6 mm diameter and 1.5 mm thickness were cleaned before being placed inside the vacuum chamber, as indicated by Pereiro et al, 2012.[27] The films were pulsed laser deposited using a UV ArF* excimer laser (Lambda Physik COMPEX 205) source ($\lambda = 193$ nm). The targets were irradiated for 15 minutes with a pulse frequency of 10 Hz and an energy density of 3.2 J.cm^{-2}. Previous to the deposition, the chamber atmosphere was evacuated down to a pressure of 10^{-5} mbar and subsequently filled with a water vapor atmosphere of 0.45 mbar. The substrates were maintained at a temperature of 460°C.

Physicochemical characterization

The morphology of the coatings was analyzed by scanning electron microscopy (SEM) using a JEOL JSM-6700F microscope and by optical profilometry using a Wyko interferometric NT 1100 microscope. Structural and compositional measurements were taken by Fourier transform infrared spectroscopy (FTIR), energy dispersive X-ray spectroscopy (EDS) and X-ray photoelectron spectroscopy (XPS). The FTIR analysis was carried out with a Bomem MB-100 spectrometer in the range of 450 to 4500 cm^{-1}. For XPS, a K-ALPHA spectrometer using monochromatic Al Kα ($h\nu = 1486.92$ eV) radiation was employed. Finally, EDS analyses were carried out with an Oxford Inca Energy 300 SEM instrument integrated in the previously mentioned SEM microscope.

hBMSCs biological response characterization

Bone marrow aspirates were obtained after informed consent from patients undergoing hip replacement surgery, at Hospital da Prelada, Porto, Portugal. Biological samples were provided under a protocol approved by the Hospital Ethical Committee and established with the 3B's Research Group. hBMSCs were isolated by gradient centrifugation followed by plastic adherence selection as previously described in Ref [28]. hBMSCS were cultured in minimum essential medium (alpha-MEM) (Sigma, USA) supplemented with 10% fetal bovine serum (FBS, Invitrogen, USA) and 1% antibiotic/antimicotics (Sigma, USA) to maintain an undifferentiated state. Coated discs, previously sterilized by gamma radiation, were placed in 48-well plates and 1 mL of a cell suspension of hBMSCs, containing 5000 cells at passage 4, was dispensed on the materials. Cultures were maintained in alpha-MEM (basal medium) and in alpha-MEM supplemented with osteogenic differentiation factors (osteogenic medium) such as 10 mM β-glycerophosphate (Sigma, USA), 150 µg/mL ascorbic acid (Sigma, USA) and 1×10^{-8} M dexamethasone (Sigma, USA), for 7, 14, 21 and 28 days in a humidified atmosphere with 5% CO_2 and at 37°C. Media were changed every 2–3 days. Three discs of each material were used per condition and time point, and tissue culture polystyrene (TCPS) was used as control of the assay for all the three independent experiments.

Cell adhesion and morphology on the Si2.5Sr2.5 and Si0Sr0 coatings was analysed by SEM by subjecting the seeded coatings to the protocol previously described by López-Álvarez et al.[29] and observed at a Philips XL30 SEM (CACTI, Universidade de Vigo). Cell proliferation was assessed by total *ds*DNA quantification along the time of culture. The osteogenic differentiation of hBMSCs and their osteogenic activity was followed by determining the activity of alkaline phosphatase (ALP), a marker of early osteogenic differentiation. Discs were carefully rinsed twice with PBS and submitted to osmotic and thermal shocks to obtain cell lysates. The *ds*DNA content of each sample was measured using the lysates and the PicoGreen dsDNA Quantification Kit (Molecular Probes) following manufacturer instructions. Fluorescence was read in a microplate reader (Bio-Tek, USA) at 485ex/525em. The *ds*DNA values were normalized against the cells growth area. The same cell lysates were used to quantify the activity of ALP enzyme using the spectrophotometric assay based on the conversion of p-nitrophenil-phosphate to p-Nitrophenol. The ALP activity values were normalized against the amount of *ds*DNA.

Statistical analysis

*ds*DNA and ALP activity data are presented as mean values ($n = 3$) and the error bars represent standard deviations. Statistical differences were evaluated by

using the analysis of variance (ANOVA) and the Student's t-test with p values <0.05 (represented as *) and <0.01 (represented as **) considered statistically significant.

Results and discussion

Physicochemical characterization

The SEM analysis has provided information about the morphology of the coatings, as well as a first semi-qualitative identification, via EDS analysis, of the elements present. At low magnification (not shown), the surface morphology of all the samples is very similar and it is constituted of aggregates of globular shape, typical of CaP films, following the topography of the titanium substrate. At higher resolution, however, some differences seem to emerge. Figure 1 shows high magnification images taken by SEM of the samples Si0Sr0 (a), Si2.5Sr0 (b) and Si2.5Sr5.0 (c), all of them being films deposited on titanium. The micrograph for the reference CaP coating (Figure 1(a)) shows a compact surface constituted by globular groupings that appear to have an important surface roughness. As a stark contrast, the representative image for the Si-doped coating (Si2.5Sr0 sample - Figure 1(b)) reveals the presence of well rounded grains with a mean diameter of 30 ± 10 nm. These grains appear to be fused to each other creating an interconnected structure. The multi-doped coating shown in Figure 1(c) reveals a similar morphology, but the grains seem to present a higher surface roughness, being more difficult to resolve these grains as independent identities. The other coatings of the series presenting a varying percentage of Sr (not shown) present surface morphologies that are transitions between these two extremes. Simultaneously to the acquisition of morphological images, EDS analyses were performed (Figure 1(d) to (f)). These analyses not only revealed the presence of elements that constitute the CaP coating (P, Ca and O), but, additionally, Si and Sr were undoubtedly identified in the multi-doped coating composition. The Sr produced clear peaks in the spectra of all the Sr-containing samples, these peaks being more intense in those coatings fabricated with a higher concentration of Sr in the target material.

A local profilometry reconstruction of the film surface of three representative samples (Si0Sr0, Si2.5Sr0 and Si2.5Sr7.5) is shown in Figure 2 (films deposited on a silicon wafer to avoid the accumulated effect of the substrate roughness). As it can be observed, the surface topographies of the three samples, and most notably the multi-doped coating, are remarkably different. The reference coating presents a low roughness surface characterized by the presence of both small

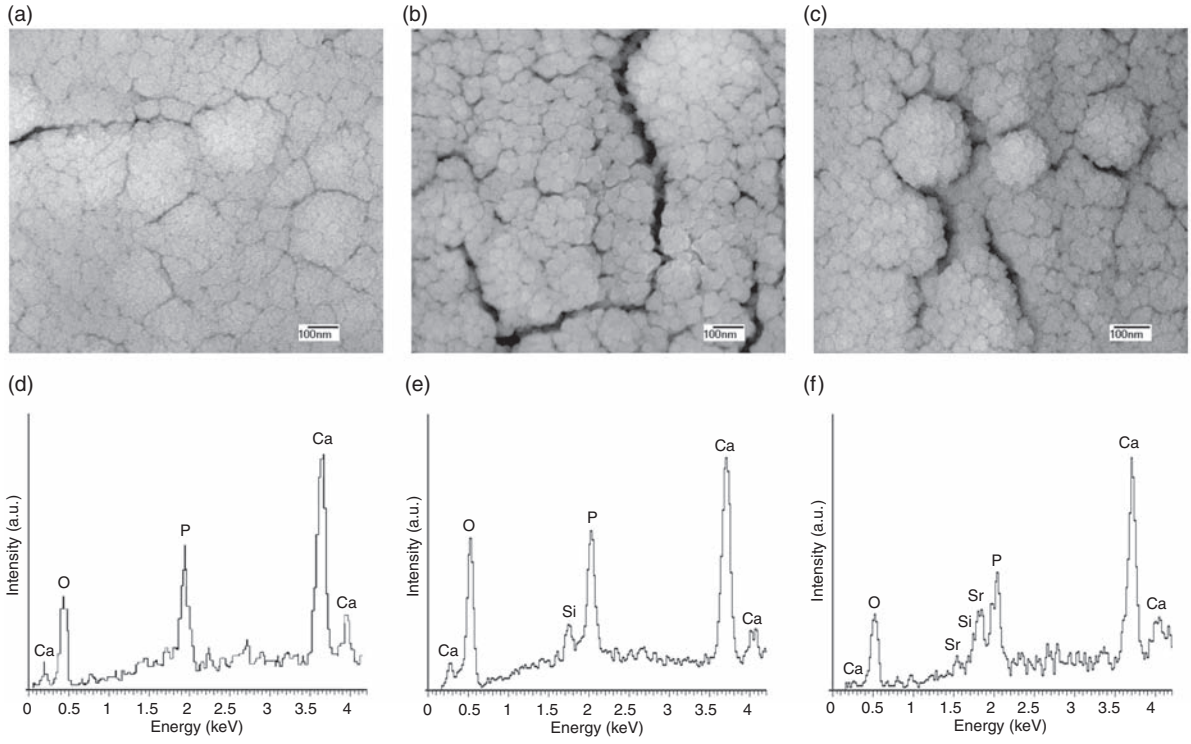

Figure 1. SEM micrographs of the coatings: Si0Sr0 (a), Si2.5Sr0 (b) and Si2.5Sr5.0 (c) at high magnification and their respective EDS spectra (d–f).

irregularities and crater-like structures most probably a result of the impact of droplets ejected from the target material. In contrast, the sample fabricated from a target material containing a 2.5 at.% Si but no Sr presents a smoother surface lacking the presence of these crater-like irregularities. Finally, the sample produced from the target containing both 2.5 at.% Si and 7.5 at.% Sr shows a much higher surface roughness presenting irregularities in a wide range of sizes including crater-like structures. These extreme values of Si2.5Sr0 and Si2.5Sr7.5 were chosen to ensure the evaluation of the contribution of both elements separately on the roughness, as intermediate values could not provide clear information for this purpose. These differences are reflected in the obtained values for the root mean square roughness (Rq) of the three samples: 67.8 nm for the reference coating (Si0Sr0), 26.3 nm for the sample containing Si (Si2.5Sr0) and 128.5 nm for the multi-doped one (Si2.5Sr7.5). On the other hand, the depth analysis, performed in the cavity left by the removal of a dry silver solution drop, revealed a ratio of deposition of $43.2\,nm \times min^{-1}$ for Si0Sr0, $24.5\,nm \times min^{-1}$ for Si2.5Sr0 and $33.2\,nm \times min^{-1}$ for Si2.5Sr7.5, values that agree well with the amount of crater-like structures present in the surface of the coatings.

Figure 3(a) shows the FTIR spectra of all the fabricated coatings, corresponding well to a carbonated CaP. The main vibration modes can be identified as: (i) phosphate groups; a strong peak located between 1000 and $1200\,cm^{-1}$ attributed to the asymmetric stretching of P-O bonds, a weak band at $950\,cm^{-1}$ due to symmetric stretching, and an absorption band between 550 and $600\,cm^{-1}$, associated with symmetric bending, (ii) carbonate groups; an absorption band between 1400 and $1500\,cm^{-1}$ attributed to the asymmetric stretching of C-O bonds and a weaker band at $870\,cm^{-1}$ due to asymmetric bending. Some differences among samples are evident from these spectra. The B spectrum of Figure 3(a) corresponds to the coating fabricated only with a 2.5 at.% Si in the target but no strontium (Si2.5Sr0). It can be observed that this has the effect of decreasing the intensity of the band attributed to the symmetric bending of CO_3^{2-} groups (with respect to the non-doped CaP, spectrum A) as well as a general lowering of the intensity and definition of all the bands. The progressive incorporation of strontium, maintaining a constant 2.5 at.% Si in the target composition, as seen from the C to F spectra, leads to a progressive increase in the intensity of the carbonate bands. This phenomenon is, however, not linear, with a high increase in the intensity of this band observed for the coating obtained from a 7.5% Sr target (Si2.5Sr7.5). To quantify this phenomenon and avoid the possibility of total intensities being correlated to other parameters other than the density of the groups in the coatings, a ratio below the areas of the bands corresponding to CO_3^{2-} groups versus those of PO_4^{3-} has been calculated and represented (as a function of the sum of both the Si and Sr content) in Figure 3(b). This ratio shows a first decrease due to the incorporation of Si without Sr (Si2.5Sr0 sample), and a subsequent general increase in its value, in agreement with the incorporation of CO_3^{2-} groups from the $SrCO_3$ compound, with a very marked increase for the coating fabricated from the highest amount of $SrCO_3$. Finally, a very weak but clearly observable peak is found at $710\,cm^{-1}$. This peak has also been observed when Sr-substituted CaP coatings were obtained and is thus probably due to the presence of this element.[27]

Finally, with the purpose of evaluating the quantitative composition of the coatings, an XPS analysis has been carried out. Figure 4 shows the C_{1s}, Sr_{3p} and Si_{2p} high resolution XPS spectra for the coatings obtained from targets with different Sr contents and a constant percentage of Si at 2.5 at.%. The increase in intensity of the Sr_{3p} signal is most evident, being correlated with the increase of $SrCO_3$ in the target material. Less evident is the increase of the C_{1s} signal associated with carbonate

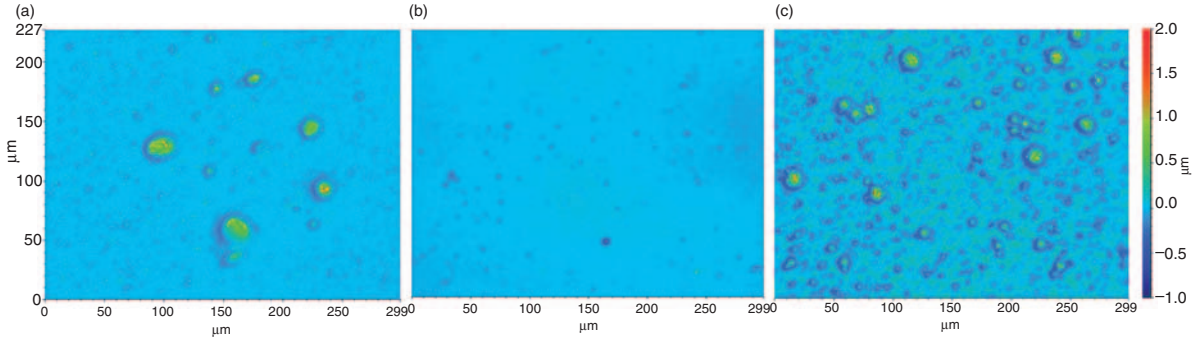

Figure 2. Surface topography reconstructions by optical profilometry of the coatings: Si0Sr0 (a), Si2.5Sr0 (b) and Si2.5Sr7.5 (c). The films were deposited on Si substrates.

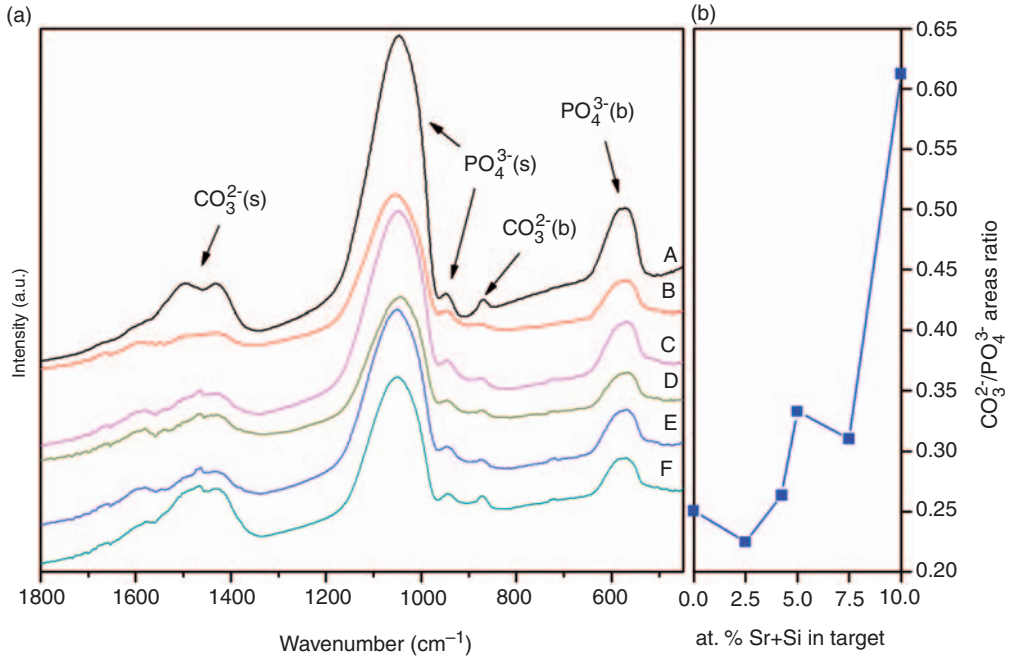

Figure 3. (a) FTIR spectra of the coatings: (A) Si0Sr0, (B) Si2.5Sr0, (C) Si2.5Sr1.75, (D) Si2.5Sr2.5, (E) Si2.5Sr5.0 and (F) Si2.5Sr7.5. and (b) CO_3^{2-}/PO_4^{3-} areas ratio obtained from the spectra.

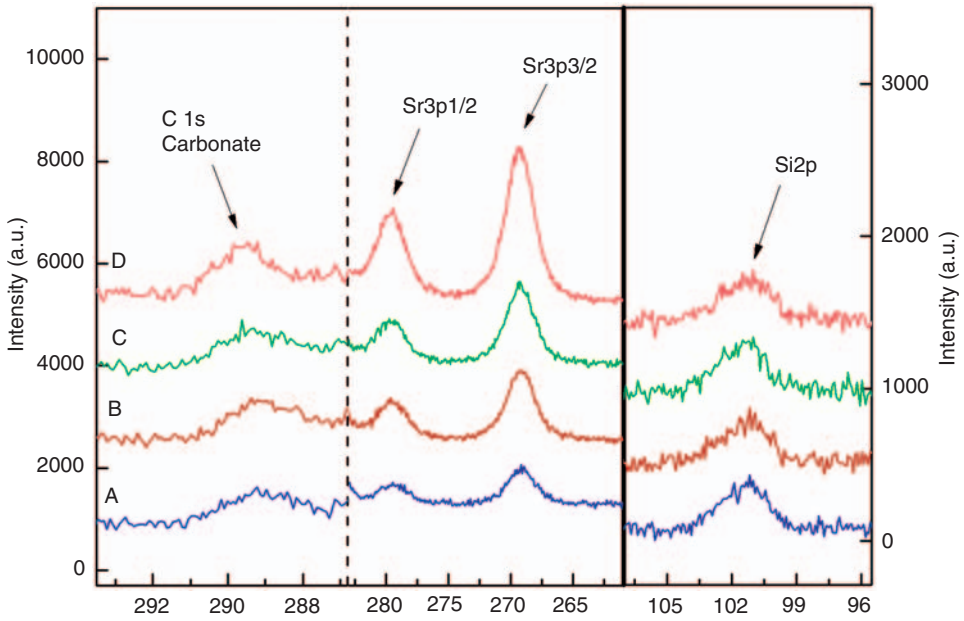

Figure 4. High resolution XPS spectra of the C_{1s} associated to carbonate groups (a), Sr_{3p} (b) and Si_{2p} (c) electronic transitions, for: (A) Si2.5Sr1.75, (B) Si2.5Sr2.5, (C) Si2.5Sr5.0, (D) RSr2.5Si7.5.

groups, which only shows a clear increase for the coating fabricated with the highest amount of Sr (Si2.5Sr7.5), in agreement with the spectra obtained by FTIR. The quantitative evaluation of the at.% of Ca, P, O, C, Si and Sr is shown in Table 2. As seen, the incorporation of C shows a pattern that follows the one obtained for the CO_3^{2-}/PO_4^{3-} ratio by FTIR (Figure 3(b)), with a first decrease from 2.4 to 1.4 at.% C and a following increase with the increasing presence of $SrCO_3$ in the target material. On the

Table 2. X-ray photoelectron spectroscopy (XPS) analysis of the coatings.

	Elemental composition (at.%)						Binding energy (±0.2 eV)				
Coating	$C(CO_3^2)$	O	Ca	P	Si	Sr	Ca_{2p}	P_{2p}	O_{1s}	Si_{2p}	Sr_{3p}
Si0Sr0	2.4	44.1	18.8	10.6	0.0	0.0	347.5	133.6	531.5	–	–
Si2.5Sr0	1.4	44.2	17.6	10.7	2.5	0.0	347.5	133.5	531.4	102.0	–
Si2.5Sr1.75	2.3	45.0	16.6	9.7	2.8	0.9	347.3	133.4	531.1	101.7	269.4
Si2.5Sr2.5	2.6	44.1	15.7	10.8	1.6	2.0	347.3	133.4	531.1	101.6	269.4
Si2.5Sr5.0	2.7	46.0	15.8	10.9	2.3	2.4	347.3	133.3	531.1	101.6	269.3
Si2.5Sr7.5	3.1	47.6	14.8	11.7	1.9	4.3	347.3	133.4	531.2	101.4	269.3

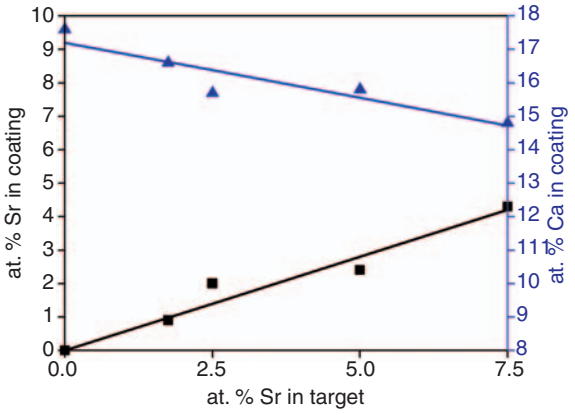

Figure 5. Sr (■) and Ca (▲) at. % in the coatings obtained by XPS as a function of the at. % Sr in the target.

other hand, the values for Si in the coatings seem to vary around their expected value of 2.5 at.% for low concentrations of $SrCO_3$ in the target, apparently diminishing for higher concentrations (Table 2). A progressive increase in the Sr content incorporated in the coatings can be observed with the increase in the $SrCO_3$ content of the target material. At the same time, as the content of Sr increases with the increase of $SrCO_3$ in the target material, the Ca content is shown to decrease. These values are represented in Figure 5. As observed, the Ca content decreases as the percentage of Sr increases and the linear regression of the data revealed the equations, shown below in (1) and (2), where the formulae of at.% of Sr and Ca in the coatings, respectively, are presented.

$$[\text{at. \% Sr}]_{\text{Coating}} = 0.542[\text{at. \% Sr}]_{\text{target}} + 0.105 \quad (1)$$

$$[\text{at. \% Ca}]_{\text{Coating}} = -0.330[\text{at. \% Sr}]_{\text{target}} + 17.206 \quad (2)$$

In the case of the binding energies (Table 2), the energies of the Ca_{2p}, P_{2p}, O_{1s} peaks are all equivalent, within experimental error, to the energies found for the reference coating (Si0Sr0). The values for strontium reveal that it is being incorporated as Sr^{2+} ions, while the values for silicon can be attributed to orthosilicate groups SiO_4^{4-}(101.6 eV), diminishing slightly with the incorporation of $SrCO_3$ in the coatings.[30]

From the results obtained by both FTIR and XPS, it appears that all the coatings present a similar structure, undoubtedly identified as a carbonated CaP. The XPS results show that the P2p and O1s binding energy peaks are centered at 133.4 ± 0.2 eV and 531.1 ± 0.2 eV, respectively (Table 2), being these energies assignable to CaP groups.[31] Additionally, the Ca2p and P2p binding energies for the coating of the series are all very similar to the values found in the reference non-doped coating. This is in agreement with the results from previous studies, where the incorporation of metallic silicon, diatomeas earth and strontium carbonate[26,27] has been demonstrated.

On the other hand, the profilometry analysis for Si2.5Sr0 seems to suggest that the presence of the elements of the diatomaceous earth (Si, Mg, Na, Al, K, Fe) in the irradiated target has an attenuation effect on the final surface roughness of the coating as well as a significant decrease on the rate of deposition. It is important to clarify that the composition of this coating (Si2.5Sr0) has been previously evaluated by Solla et al.,[32] where concentrations of Na (0.06 at.%), Mg (0.3 at.%), Al (0.3 at.%), K (0.04 at.%) and Fe (0.08at.%) were estimated. In case of multi-doped coatings, they presented a much higher Rq than Si-doped or non-doped coatings, in spite of its lower rate of deposition as compared to the reference carbonated CaP coating. Interestingly, Sr-doped carbonated CaP coatings did not show an increase in surface roughness with the increase in Sr content in a previous study.[27] This suggests that both $SrCO_3$ and diatomaceous earth need to be present for this to occur. This apparent increase in surface roughness is also evident by SEM (increased surface roughness of the globular groupings, compare

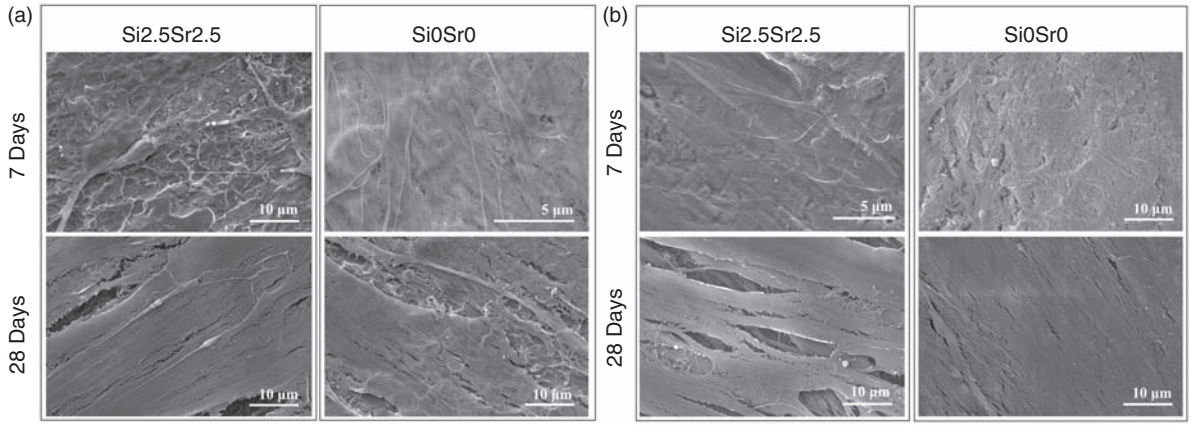

Figure 6. SEM micrographs showing the morphology of hBMSCs on the surface of the Si2.5Sr2.5 and Si0Sr0 coatings, after 7 and 28 days of culture in alpha-MEM medium (a) and alpha-MEM supplemented with osteogenic factors (b).

Figure 1(b) and (c)) and represents a positive phenomenon, as an increased nano-roughness is generally considered to be an enhancer of the bioactivity of coatings by increasing the cells attachment to the surface.[33,34]

The XPS and FTIR analyses show what appears to be a complex interaction between the elements that constitute the diatomaceous earth and $SrCO_3$. The comparison between Si0Sr0 and Si2.5Sr0 coatings reveals a reduction in carbonate groups by FTIR that is confirmed by the reduction of the calculated at.% of C attributed to carbonate groups by XPS. As mentioned before, the binding energy for the Si_{2p} peak (Table 2) corresponds to orthosilicates.

In previous studies,[27] using only $SrCO_3$ to produce CaP coatings by PLD, XPS results suggest a substitution mechanism in the CaP structure of Sr^{2+} in place of Ca^{2+}. This preference of Sr^{2+} for Ca^{2+} sites has already been reported in other studies of Sr-substituted hydroxyapatite obtained by other methods.[35,36] Due to the smaller size of the Ca^{2+} with respect to Sr^{2+} (Ca^{2+} ionic radius = 0.100 nm; Sr^{2+} ionic radius = 0.118 nm), changes in the CaP composition are expected.

In the case of the present study, not only $SrCO_3$ is used but also diatomaceous earth. Thus, although there may be a substitution process of Sr^{2+} in place of Ca^{2+}, the presence of Si and other elements from diatomaceous earth causes a more complex process. This process has been named in this work as doping.

As it was already published,[32] the effective incorporation of at.% of Na, Mg, Al, K and Fe into the CaP coatings could eventually lead to a better biological performance. The incorporation of these ions in the CaP coatings occurs most probably either in the form of interstitial doping or occupying the place of Ca^{+2} in the case of alkaline earth metals and perhaps also of alkali metals due to their similar chemical properties.

hBMSCs response characterization

To evaluate the hBMSCs response on Si-Sr-carbonated CaP coatings, we have selected the Si2.5Sr2.5 ones (real coating doping on HA of 1.6 at.% Si and 2.0 at.% Sr) because of the bibliography values found where Si ranging from 0.8 to 1.6% by weight incorporated into CaP coatings contributed to an enhanced bioactivity of the coatings[37] and, in case of Sr, optimum values for the best osteoblastic response were found between 1 and 10 at.%.[38,39]

Morphology of hBMSCs seeded on the Si2.5Sr2.5 and Si0Sr0 coatings (as control) analyzed by SEM after 7 and 28 days of culture in alpha-MEM medium (basal medium) and alpha-MEM medium supplemented with osteogenic factors (osteogenic medium) is presented in Figure 6. Thus, after 7 days of culture, adherent cells were observed on both coatings and on both media (basal in Figure 6(a) and osteogenic in (b)) presenting the typical flat morphology of hBMSCs adapting perfectly to the coatings topography. Interactions between cells and both coatings can be observed. As the whole surfaces were not entirely covered by a layer of cells, filopodia and lamellipodia projected by cells can be distinguished. No differences were observed concerning the morphology of cells between the two coatings, the multi-doped coating (Si2.5Sr2.5) and the control coating (Si0Sr0), in any of the media. After 28 days of incubation the surfaces of both coatings on both media appeared completely covered by a thick layer of cells indicating that none of the coatings had a deleterious effect on cell adhesion or proliferation.

In what concerns to cell proliferation, *ds*DNA was quantified along the time of culture in both media and it is represented in Figure 7. The amount of *ds*DNA, directly correlated to the number of cells, in basal

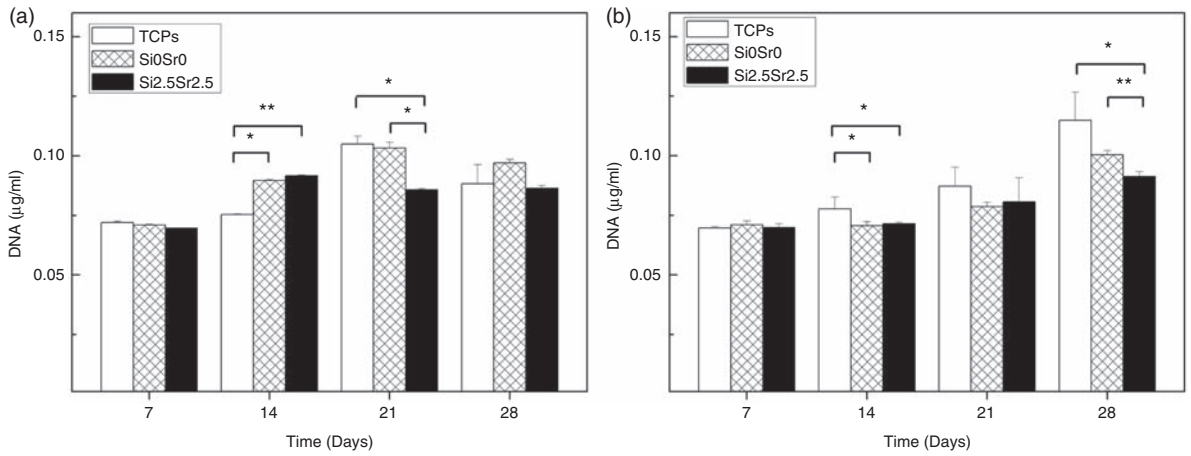

Figure 7. Amount of *ds*DNA of hBMSCs cultured up to 28 days on the Si2.5Sr2.5 and Si0Sr0 coatings in alpha-MEM medium (a) and alpha-MEM supplemented with osteogenic factors (b). TCPS was used as control of the experiment.

medium (Figure 7(a)) and for both coatings and the experimental control TCPS (tissue cultured polystyrene), showed the same *ds*DNA amount for all tested samples at day 7, a steady increase up to day 21, except in Si2.5Sr2.5 up to day 14, followed by a slight decrease up to 28 days, except again in multi-doped coating where amount of *ds*DNA was constant compared to day 21. Significant lower amount of *ds*DNA was found in TCPS than on non-doped ($p < 0.05$) and multi-doped ($p < 0.01$) coatings at day 14 and in Si2.5Sr2.5 than on TCPS and Si0Sr0 at day 21($p < 0.05$). The hBMSCs proliferation under osteogenic conditions (Figure 7(b)) presented the same *ds*DNA amount at day 7 for all tested samples and with similar values than on basal medium (Figure 7(a)). The cell proliferation rate was in general lower than in basal medium, with a continuous but less intense increase at *ds*DNA values at 14 and 21 days for all samples. The amount of *ds*DNA was clearly higher at day 28, with important increase in all tested materials but especially in TCPS. Significantly higher ($p < 0.05$) amount of *ds*DNA was found in TCPS at day 14 compared to both coatings and at day 28 compared to multi-doped coating ($p < 0.05$). At the same time, the amount of *ds*DNA was significantly higher ($p < 0.01$) in Si0Sr0 compared to multi-doped coating at day 28. It is of relevance to clarify that in both coatings the dsDNA values are underestimated with respect to the TCPS as a result of measuring a smaller area of cell layer (TCPS area/well 0.785cm^2 and coating area/well was 0.565 cm^2).

The osteogenic differentiation of hBMSCs was evaluated by the quantification of the activity of the ALP enzyme along the time of culture in both media (Figure 8). The ALP values detected for both coatings and TCPS on basal medium (Figure 8(a)) remained practically constant along the time of culture. Despite the significantly higher ($p < 0.01$) ALP activity in both coatings in comparison to TCPS at days 14 and 28 (being for this day $p < 0.01$ for non-doped coating and $p < 0.05$ for multi-doped), hBMSCs did not differentiate towards the osteogenic lineage when cultured in basal medium with the unique stimulation of the morphology and composition of the coatings. Contrarily, when hBMSCs were cultured in osteogenic medium (Figure 8(b)), the ALP activity values dramatically increased at 21 days on both coatings to remain at these values after 28 days. Again, at days 21 and 28, cells on both coatings presented significantly higher ($p < 0.01$) enzymatic activity than on TCPS. At the same time, at 28 days the ALP activity was significantly higher ($p < 0.05$) on Si2.5Sr2.5 coatings compared to non-doped ones.

In view of the results obtained when evaluating the biological behaviour for hBMSCs on the tested Si2.5Sr2.5 coatings, the outcome was clearly favourable and had no negative impact on the cells. Moreover, it has been published that as a consequence of the doping of the CaP coatings with other elements, it will be expected to have an increase in the release of silicon and strontium to the extracellular medium.[40–42] This could, in turn, have a stimulating effect on cells with increased interactions between them and the coating, something already shown by Pietak et al.,[41] who concluded that Si-doped implants improved the biological activity of osteoblasts due to the Si release into the extracellular medium. Thus, the presence of this Si in the culture medium, in a controlled rate, was hypothesized to affect the regulators of DNA synthesis in the human osteoblast-like cells and, in turn, to have stimulatory effects on the bone mineralization process.[43] In the present work, the possible release of both elements (Si and Sr) into the culture medium can have influenced the great behaviour of cells in terms of early

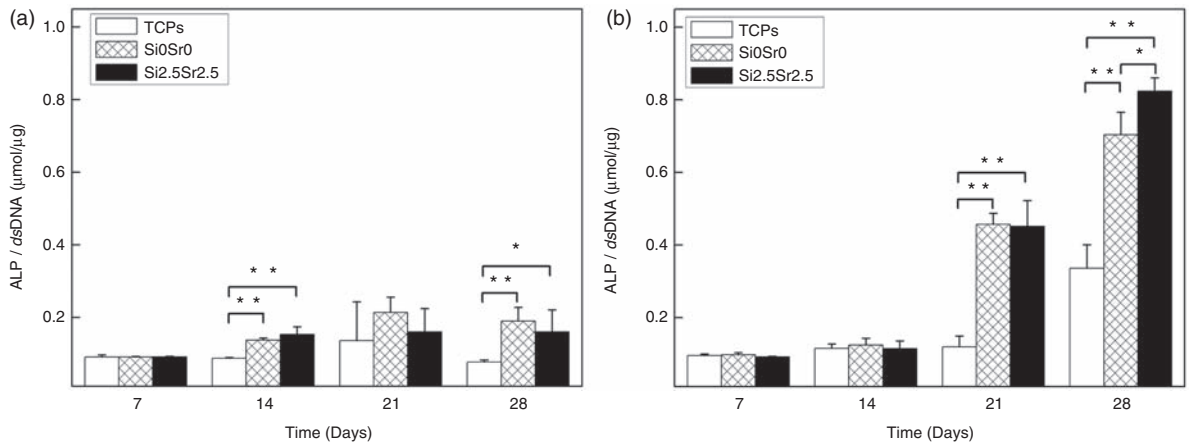

Figure 8. ALP activity normalized to the amount of *ds*DNA in hBMSCs cultured up to 28 days on the Si2.5Sr2.5 and Si0Sr0 coatings in alpha-MEM medium (a) and alpha-MEM supplemented with osteogenic factors (b). TCPS was used as the control of the experiment.

differentiation (ALP synthesis, Figure 8), as it was previously reported in case of Si-CaP coatings.[29] On the other hand, Xue et al.[39] demonstrated that the presence of Sr stimulates osteogenic differentiation and encourages the osteoblastic activity. At the same time, the presence of Si or Sr in CaP coatings was shown to improve osteoblasts proliferation and bone extracellular matrix production[44] as well as to stimulate the osteoblastic activity and inhibit osteoclast proliferation.[38] Finally, although an in-depth cell study will be performed to elucidate the independent effects of both ions on the behaviour of the hBMSCs, the results obtained suggested that the proposed multi-doped Si2.5Sr2.5 coatings promoted higher levels of early differentiation of hBMSCs to osteoblasts.

Conclusions

The obtaining of multi-doped coatings of carbonated CaP with silicon and strontium by PLD technique was demonstrated. The technique was proven to allow an accurate control of the atomic percentages of Si and Sr at the doped coatings. The multi-doped coatings were demonstrated to present the typical globular morphology of CaP and increased nano-roughness. The healthy proliferation of hBMSCs up to 28 days on Si2.5Sr2.5 coatings was proven together with their significantly higher early differentiation in osteogenic medium at 21 days when compared to TCPS and at 28 days when compared to both the TCPS and the non-doped coating.

Acknowledgements

Technical staff of CACTI (University of Vigo) is gratefully acknowledged. This work was partially supported by the UE-POCTEP 0330IBEROMARE1P project, UE-INTERREG 2011-1/164MARMED and Ministerio de Ciencia e Innovación (Project MAT2010-18281). M López-Álvarez thanks funding support from FP7/REGPOT-2012-2013.1 (n°316265, BIOCAPS).

References

1. Hench LL. Bioactive ceramics. In: Ducheyne P, Lemons JE (eds) *Bioceramics: material characteristics versus in vivo behavior*. New York: Annals of The New York Academy of Sciences, 1998, pp.54–71.
2. Campbell AA. Bioceramics for implant coatings. *Mater Today* 2003; 6: 26–30.
3. Long M and Rack HJ. Titanium alloys in total joint replacement - a materials science perspective. *Biomaterials* 1998; 19: 1621–1639.
4. Klein CPAT, Patka P, Wolke JGC, et al. Long-term in vivo study of plasma-sprayed coatings on titanium alloys of tetracalcium phosphate, hydroxyapatite and α-tricalcium phosphate. *Biomaterials* 1994; 15: 146–150.
5. Voigt JD and Mosier M. Hydroxyapatite (HA) coatings appears to be of benefit for implant durability of tibial components in primary total knee arthroplasty. *Acta Orthopaedica* 2011; 82: 448–459.
6. Narayanan R, Seshadri SK, Kwon TY, et al. Calcium phosphate-based coatings on titanium and its alloys. *J Biomed Mater Res Part B: Appl Biomater* 2008; 85: 279–299.
7. Ripamonti U, Roden LC and Renton LF. Osteoinductive hydroxyapatite-coated titanium implants. *Biomaterials* 2012; 33: 3813–3823.
8. García-Sanz FJ, Mayor MB, Arias JL, et al. Hydroxyapatite coatings: a comparative study between plasma-spray and pulsed laser deposition techniques. *J Mater Sci: Mater Med* 1997; 8: 861–865.
9. Mayor MB, Arias JL, García-Sanz FJ, et al. Producción de recubrimientos de fosfato cálcico mediante ablación láser para aplicaciones biomédicas. *Rev Metalurg* 1998; 34: 89–93.

10. Wang G and Zreiqat H. Functional coatings or films for hard-tissue applications. *Materials* 2010; 3: 3994–4050.
11. Fernández-Pradas J, García-Cuenca M, Clèries L, et al. Influence of the interface layer on the adhesion of pulsed laser deposited hydroxyapatite coatings on titanium alloy. *Appl Surf Sci* 2002; 195: 31–37.
12. García-Sanz FJ, Mayor MB, Arias JL, et al. Hydroxyapatite coatings: a comparative study between plasma-spray and pulsed laser deposition techniques. *J Mater Sci Mater Med* 1997; 8: 861–865.
13. León B. Pulsed laser deposition of thin calcium phosphate coatings. In: León B, Jansen JA (eds) *Thin calcium phosphate coatings for medical implants*. New York: Springer, 2009, pp.101–155.
14. Mihailescu IN, Torricelli P, Bigi A, et al. Calcium phosphate thin films synthesized by pulsed laser deposition: physico-chemical characterization and in vitro cell response. *Appl Surf Sci* 2005; 248: 344–348.
15. Peraire C, Arias JL, Bernal D, et al. Biological stability and osteoconductivity in rabbit tibia of pulsed laser deposited hydroxylapatite coatings. *J Biomed Mater Res A* 2006; 77: 370–379.
16. Carlisle EM. Biochemical and morphological changes associated with long bone abnormalities in silicon deficiency. *J Nutr* 1980; 110: 1046–1056.
17. Nielsen FH and Sandstead HH. Are nickel, vanadium, silicon, fluorine, and tin essential for man? a review. *Am J Clin Nutr* 1974; 27: 515–520.
18. Xynos ID, Edgar AJ, Buttery LD, et al. Gene-expression profiling of human osteoblasts following treatment with the ionic products of Bioglass 45S5 dissolution. *J Biomed Mater Res* 2001; 55: 151–157.
19. Sripanyakorn S, Jugdaohsingh R, Thompson RPH, et al. Dietary silicon and bone health. *Nutr Bull* 2005; 30: 222–230.
20. Sowden EM and Stitch SR. Trace elements in human tissue. Estimation of the concentrations of stable strontium and barium in human bone. *Biochem J* 1957; 67: 104–109.
21. Hodges RM, MacDonald NS, Nusbaum R, et al. The strontium content of human bones. *J Biol Chem* 1950; 185: 519–524.
22. Pors Nielsen S. The biological role of strontium. *Bone* 2004; 35: 583–588.
23. Canalis E, Hott M, Deloffre P, et al. The divalent strontium salt S12911enhances bone cell replication and bone formation in vitro. *Bone* 1996; 18: 517–523.
24. Chang W, Tu C, Chen TH, et al. Expression and signal transduction of calcium-sensing receptors in cartilage and bone. *Endocrinology* 1999; 140: 5883–5893.
25. Marie PJ, Hott M, Modrowski D, et al. An uncoupling agent containing strontium prevents bone loss by depressing bone resorption and maintaining bone formation in estrogen-deficient rats. *J Bone Miner Res* 1993; 8: 607–615.
26. Solla EL, Borrajo JP, González P, et al. Study of the composition transfer in the pulsed laser deposition of silicon substituted hydroxyapatite thin films. *Appl Surf Sci* 2007; 253: 8282–8286.
27. Pereiro I, Rodríguez-Valencia C, Serra C, et al. Pulsed laser deposition of strontium-substituted hydroxyapatite coatings. *Appl Surf Sci* 2012; 258: 9192–9197.
28. Wolfe M, Pochampally R, Swaney W, et al. Isolation and culture of bone marrow-derived human multipotent stromal cells (hMSCs). *Methods Mol Biol* 2008; 449: 3–25.
29. López-Álvarez M, Solla EL, González P, et al. Silicon–hydroxyapatite bioactive coatings (Si–HA) from diatomaceous earth and silica. Study of adhesion and proliferation of osteoblast-like cells. *J Mater Sci Mater Med* 2009; 20: 1131–1136.
30. Balas F, Pérez-Pariente J and Vallet-Regí M. In vitro bioactivity of silicon-substituted hydroxyapatites. *J Biomed Mater Res A* 2003; 66: 364–375.
31. Casaletto MP, Kaciulis S, Mattogno G, et al. XPS characterization of biocompatible hydroxyapatite–polymer coatings. *Surf Interface Anal* 2002; 34: 45–49.
32. Solla EL, González P, Serra J, et al. Pulsed laser deposition of silicon substituted hydroxyapatite coatings from synthetical and biological sources. *Appl Surf Sci* 2007; 254: 1189–1193.
33. Mendonça G, Mendonça DBS, Simões LGP, et al. The effects of implant surface nanoscale features on osteoblast-specific gene expression. *Biomaterials* 2009; 30: 4053–4062.
34. Nishimura I, Huang Y, Butz F, et al. Discrete deposition of hydroxyapatite nanoparticles on a titanium implant with predisposing substrate microtopography accelerated osseointegration. *Nanotechnology* 2007; 18: 245101.
35. O'Donnell MD, Fredholm Y, de Rouffignac A, et al. Structural analysis of a series of strontium-substituted apatites. *Acta Biomater* 2008; 4: 1455–1464.
36. Boanini E, Gazzano M and Bigi A. Ionic substitutions in calcium phosphates synthesized at low temperature. *Acta Biomater* 2010; 6: 1882–1894.
37. Huang J, Jayasinghe SN, Best SM, et al. Novel deposition of nano-sized silicon substituted hydroxyapatite by electrostatic spraying. *J Mater Sci Mater Med* 2005; 16: 1137–1142.
38. Capuccini C, Torricelli P, Sima F, et al. Strontium-substituted hydroxyapatite coatings synthesized by pulsed-laser deposition: in vitro osteoblast and osteoclast response. *Acta Biomater* 2008; 4: 1885–1893.
39. Xue W, Hosick HL, Bandyopadhyay A, et al. Preparation and cell–materials interactions of plasma sprayed strontium-containing hydroxyapatite coating. *Surf Coatings Technol* 2007; 201: 4685–4693.
40. Chen D, Fu Y, Gu G, et al. Preparation and solubility of the solid solution of strontium substituted hydroxyapatite. *Chin J Biomed Eng* 2001; 20: 278–280.
41. Pietak AM, Reid JW, Stott MJ, et al. Silicon substitution in the calcium phosphate bioceramics. *Biomaterials* 2007; 28: 4023–4032.
42. Zhang W, Shen Y, Pan H, et al. Effects of strontium in modified biomaterials. *Acta Biomater* 2011; 7: 800–808.
43. Thian ES, Huang J, Best SM, et al. Silicon-substituted hydroxyapatite: The next generation of bioactive coatings. *Mater Sci Eng C* 2007; 27: 251–256.
44. Hench LL. The story of Bioglass®. *J Mater Sci Mater Med* 2006; 17: 967–978.